

Reactions of Sodium Clusters with Water Clusters

L. Bewig,[†] U. Buck,* S. Rakowsky,[‡] M. Reymann,[§] and C. Steinbach

Max-Planck-Institut für Strömungsforschung, Bunsenstrasse 10, D-37073 Göttingen, Germany

Received: August 26, 1997; In Final Form: November 21, 1997

In a crossed molecular beam experiment, the reactive scattering of sodium clusters Na_n ($n \leq 21$) with water clusters $(\text{H}_2\text{O})_m$ ($m \leq 40$) is investigated. By measuring the angular and the velocity distributions of the scattered reaction products, direct information on the reaction mechanisms is obtained. The sodium clusters are generated in a supersonic expansion of sodium vapor from an oven with a refilling system with argon carrier gas. The products are detected by photoionization at wavelengths of 308 and 355 nm and mass analyzed in a time-of-flight mass spectrometer (TOF-MS). In addition, a fast chopper with a pseudorandom sequence modulating the sodium cluster beam allows us to determine at the same time the velocity distributions of the products. The scattering of Na clusters with H_2O clusters shows only one series of reaction products, that is, solvated sodium atoms $\text{Na}(\text{H}_2\text{O})_m$ ($m \leq 32$) with maximum intensities at $m = 4, 5, 6$. For all products, the measured angular and velocity distributions exhibit the formation of a complex that is stabilized by isotropic evaporation of water molecules. The detected products have low translational energy. Products containing NaOH have not been observed.

1. Introduction

Alkali metal clusters belong to the best studied systems with respect to their electronic structure and optical properties.¹ In contrast, the chemical reactivity is much less investigated. Notable exceptions are the reactions of alkali metal clusters with oxygen.^{2–6} The well-known reaction of solid sodium with liquid water, leading to solvated NaOH and molecular hydrogen,⁷ and, on the other hand, the fact that in the scattering of Na atoms with H_2O molecules no products are observed⁸ focus the interest on this reaction with clusters. Up to now experiments have only been performed with a pulsed water cluster beam seeded in argon and a sodium pickup source, an arrangement in which multiple collisions are allowed.⁹ The detected products are $\text{Na}(\text{H}_2\text{O})_n$ and to a much lesser extent $\text{Na}_2(\text{H}_2\text{O})_n$. The products $\text{Na}(\text{H}_2\text{O})_n$ have further been investigated concerning their ionization potentials (IP) and neutral dissociation energies.^{9,10} Theoretical work has been conducted on the complexes $\text{Na}(\text{H}_2\text{O})_n$ and the corresponding ions.^{11–13} The two recent calculations come to the conclusion that for sizes $n \geq 4$ the IP is nearly constant as is also found in the experimental data.¹⁰ By the solvation of a sodium atom, the IP of the water clusters (3.2 eV for $\text{Na}(\text{H}_2\text{O})_n$, $n \geq 4$) is lowered even below that of the Na atoms (5.14 eV). It was now our interest to perform an experiment in the tradition of the classical crossed molecular beams in which the reaction mechanisms are deduced from a careful measurement of the angular and the velocity distribution of the reaction products.^{14,15} In the present paper we describe and analyze such a complete experiment for the scattering of $\text{Na}_n + (\text{H}_2\text{O})_m$ over a size range $n \leq 21$, $m \leq 40$. In these experiments, only products are detected that are formed in single

collision and a short time scale. In this way the results will answer the question of which state of the reaction is reached under the given conditions. We only find one type of product, namely $\text{Na}(\text{H}_2\text{O})_n$, $2 \leq n \leq 32$, with maximum intensity at $n = 4, 5, 6$. For more than 10 of these products we measured the angular and for six of them, in addition, the velocity distribution. For that purpose we used the crossed molecular beam machine described previously.^{6,16} To make the detection of a large number of products of a chemical reaction feasible, we replaced the quadrupole mass filter by a time-of-flight mass spectrometer (TOF-MS) which allows us to measure, at the same time, the velocity by time-of-flight analysis using the pseudorandom chopping technique.¹⁷ In this way we get all the products in one measurement together with their velocity. The remaining question of the specification of the reactants that start as a distribution can partly be answered by the kinematic and energetic constraints of this well-defined experiment. Energetically most of the Na cluster reactions with H_2O clusters leading to $\text{Na}(\text{H}_2\text{O})_n$ are endothermic so they can be excluded. Other products have not been detected under the present size range and conditions. The emphasis of the present experiment will be on the elucidation of the reaction mechanism, the distribution of the energy, and the size dependence of the sodium atom solvation. We start with a short description of the experimental setup in section 2, present the results in section 3, and discuss the implications in section 4.

2. Experiment

The experiment was performed in a universal crossed molecular beams machine which is described elsewhere.^{16,18} A scheme is shown in ref 6. Briefly, a seeded supersonic Na cluster beam was crossed at 90° with a pure H_2O cluster beam in a vacuum chamber under single-collision conditions. The scattered products were resolved and detected by a time-of-flight mass spectrometer (TOF-MS) applying pulsed UV-laser photoionization.¹⁷ The ionization region is located 37.4 cm downstream from the collision region. In addition, a quadrupole

[†] Present address: Auer SOG Glaswerke, Hildesheimer Str. 39, D-37581 Bad Gandersheim.

[‡] Present address: Robert-Rössle-Klinik, OP 2000, Lindenberger Weg 80, D-13122 Berlin.

[§] Present address: Institut für Physik der Technischen Universität, D-09107 Chemnitz.

* Corresponding author.

TABLE 1: Measured Laboratory Velocities of Water Clusters (H₂O)_n and the Resulting Energy and the Center-of-Mass (cm) Data in the Collision with Na of the Velocity $v = 1406 \text{ m s}^{-1}$

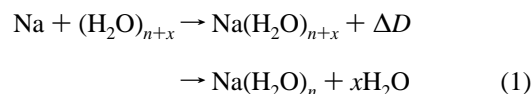
cluster size n	velocity, m s^{-1}	collision energy, meV	angle of cm, deg	velocity of cm, m s^{-1}
1	1473	217	39.4	1020
2	1392	285	57.2	1011
3	1375	323	66.5	1052
4	1342	341	71.5	1073
5	1317	353	74.7	1087
6	1302	361	77.0	1101
7	1285	366	78.7	1108
8	1277	371	80.0	1118
9	1269	374	81.1	1125
10	1260	377	81.9	1129
11	1241	376	82.5	1121
12	1249	381	83.2	1137

mass spectrometer equipped with an electron bombardment ionizer was used for the mass and velocity analysis of the direct H₂O cluster beam. Both detectors can be rotated in the plane defined by the sodium and water beams, enabling us to measure the product angular distributions in an angular range from -3° to 92° with respect to the Na cluster beam. We note that the TOF-MS is of crucial importance for the detection of the product masses. In cluster reactions these are usually unknown in advance, and in our arrangement we get them all within one sequence. In addition, the measurement of the mass information was coupled to the measurement of the velocity distributions of the products using a fast mechanical chopper (1000 Hz) with a pseudorandom (PR) sequence modulating the sodium cluster beam. By detecting the masses in each channel of the pseudorandom sequence and a subsequent deconvolution of the two-dimensional array of mass and velocity information, we simultaneously measure the TOF distributions for all products.¹⁷ The sodium cluster source and the liquid metal refilling system have been described by Bewig et al.¹⁹ The sodium clusters were generated in a supersonic expansion of sodium vapor from an oven heated to 780°C with 2 bar of argon carrier gas. To obtain a stable cluster beam, the $120 \mu\text{m}$ diameter nozzle was kept at a temperature sufficiently higher than the oven, typically at 980°C . Under these conditions, sodium clusters Na_n with $n \leq 21$ were produced. The H₂O clusters were generated in a supersonic expansion of H₂O vapor from an oven heated to 175°C , corresponding to a pressure of 10 bar. Here the $70 \mu\text{m}$ diameter nozzle was kept at 220°C . The water cluster source can also be refilled externally by excess pressure of rare gas. Therefore, the source needs not to be cooled before refilling it. Thus, water clusters with $n \leq 40$ were produced. The velocities of the beams varied between 1473 m s^{-1} for H₂O and 1241 m s^{-1} for (H₂O)₁₁ and between 1413 m s^{-1} for Na₃ and 1305 m s^{-1} for Na₁₅. The collision energies ranged from 0.217 eV for Na + H₂O and 4.8 eV for (Na)₂₀ + (H₂O)₄₀. The beam data of some selected clusters are sampled in Table 1. For the photoionization of the products at an ionizing wavelength of 308 nm a pulsed excimer laser (Lambda Physics EMG 103 MSC) has been used. By a mirror fixed at the rotating detector unit, the excimer laser radiation was steered into the ionizing volume of the TOF-MS independent of the actual detector position. The excimer laser was operated at a repetition rate of 70 Hz for the measurement of the velocity distributions, and the pulse energy at the ionizing volume was adjusted by a focusing lens with 1000 mm focal length to 4 mJ/pulse, corresponding to a flux of 8 mJ/cm^2 . Angular distributions of the products were obtained at a repetition rate of 50 Hz. Later, a pulsed Nd:YAG laser (Quantel-Brillant) with a maximum repetition rate of 50 Hz has

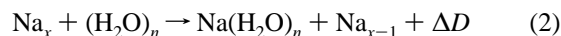
been used for photoionization at 355 nm. The compact laser head was directly fixed at the detector unit, allowing us an easier alignment of the laser output into the ionizing volume. To avoid multiphoton ionization, the output of the Nd:YAG laser has been attenuated by a telescope to a flux of 8 mJ/cm^2 . Product size distributions and angular distributions have been measured and compared at ionizing laser wavelengths of 308 and 355 nm, respectively, while the ionizing laser wavelength for product velocity distributions was set at 308 nm, exclusively.

3. Results and Analysis

The scattering of Na clusters with H₂O clusters results in the formation of Na(H₂O)_n complexes as the only reaction products observed by UV-laser photoionization. Two kinds of possible reactions have to be taken into account: the formation of complexes that are stabilized by evaporation of water molecules



and direct reactions of the type



The reaction energies ΔD are known for a number of reactions from the calculated binding energies of the reactants and the products.^{12,20-22} They range from 403 to 574 meV (exothermic) for reaction 1 and from 226 to -546 meV (mostly endothermic) for reaction 2. In addition, the internal energies of the clusters have to be considered. The temperature and thus the internal energies of the sodium clusters can be derived from the mass spectrum of the direct sodium cluster beam taken at 308 nm. The IP's of Na₄, Na₆, and Na₈ lie with 4.23 eV, 200 meV above the energy of the photons. In the mass spectrum Na₄ is hardly observed at all, whereas Na₈ is observed with an intensity similar to mass spectra taken at 266 nm which is with 4.68 eV above its IP. Thus, the internal energy of Na₈ can be estimated to be the missing 200 meV, corresponding to a temperature of the sodium cluster beam of 130 K. At this temperature, the internal energies of the clusters, depending on their numbers of degrees of freedom, range from 0 meV for the Na atoms to 600 meV for Na₂₀. These energies have to be taken into account in the energy balance of the reactions. Similar considerations hold for the water clusters, although here only a rough estimate can be given with a temperature of about $80 \pm 40 \text{ K}$. This gives for (H₂O)₇ 103 meV. We note that these clusters are solid. Because of the size distributions in the cluster beams, the reactants leading to a specific product Na(H₂O)_n are not known a priori from the experiment and have to be inferred from indirect conclusions that will be discussed later. Near the Na cluster beam only nonreactively scattered Na clusters were found, but no products. In Figure 1 the product ion intensities from a TOF mass spectrum recorded at a laboratory scattering angle of 83° with an ionizing laser wavelength of 308 nm are displayed. This angle corresponds as we will see later to a position not too far away from the maximum intensity for all product cluster sizes measured. We observe a series of complexes Na(H₂O)_n ($2 \leq n \leq 32$) centered around the main products at $n = 4, 5, \text{ and } 6$. Compared with the scattering by molecular oxygen,^{5,6} the product intensity is an order of magnitude smaller, so we have much smaller reaction cross sections in the order of 10 \AA^2 in this case.

For a correct interpretation of the data we have to take into account the ionization process. Experimentally we used dif-

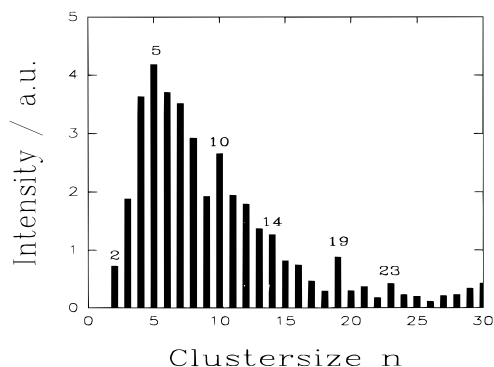


Figure 1. Product distribution of $\text{Na}(\text{H}_2\text{O})_n$ as function of cluster size measured at 83° laboratory angle by photoionization with 308 nm.

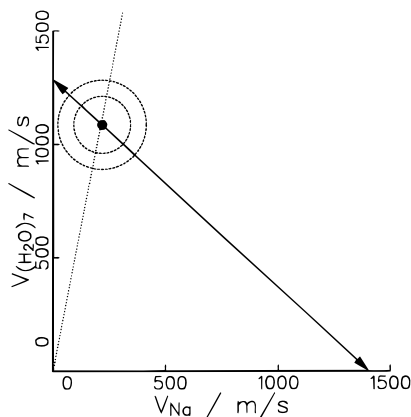
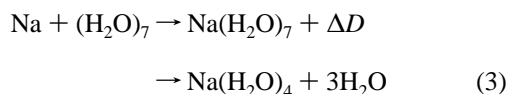


Figure 2. Newton diagram for the reaction $\text{Na} + (\text{H}_2\text{O})_7$ at a collision energy of 0.366 eV. The large circle stands for the maximum center-of-mass (cm) recoil velocity of the $\text{Na}(\text{H}_2\text{O})_4$ product. The small circle indicates the cm recoil velocity observed in the experiment.

ferent laser wavelengths to shed some light onto this problem. Compared with the product ion intensities in Figure 1, ionization with 355 nm results in a decreased intensity (relative to the intensity of $\text{Na}(\text{H}_2\text{O})_4$) for $\text{Na}(\text{H}_2\text{O})_3$, and $\text{Na}(\text{H}_2\text{O})_2$ is not observed at all. With 3.50 eV these photons just reach the IP of $\text{Na}(\text{H}_2\text{O})_3$ (3.48 eV) and not that of $\text{Na}(\text{H}_2\text{O})_2$ (3.80 eV). For the products $\text{Na}(\text{H}_2\text{O})_n$, $n \geq 4$, the IP is 3.20 eV. Therefore, the excess energy at 355 nm ionization is only 0.30 eV, whereas their ionic dissociation energies are sufficiently higher. Thus, at this wavelength no ionization-induced fragmentation takes place. At ionization with 308 nm the same angular distributions are measured as with 355 nm. So fragmentation of the products at 308 nm can also be excluded. A typical, most probable Newton diagram is shown in Figure 2 for the reaction



This reaction is exothermic with a reaction energy $\Delta D = +507$ meV, and the collision energy in the center-of-mass frame is 366 meV in our experiments. Thus, the total energy of the complex is 873 meV without and 976 meV with the internal energy of the water cluster. This allows the complex to subsequently evaporate three water molecules. The large Newton circle drawn in Figure 2 describes the possible velocities of the product $\text{Na}(\text{H}_2\text{O})_4$ for zero internal excitation of the product. The small circle stands for an appreciable internal excitation or small translational energies. The values correspond to the experimental result (see the later discussion). The

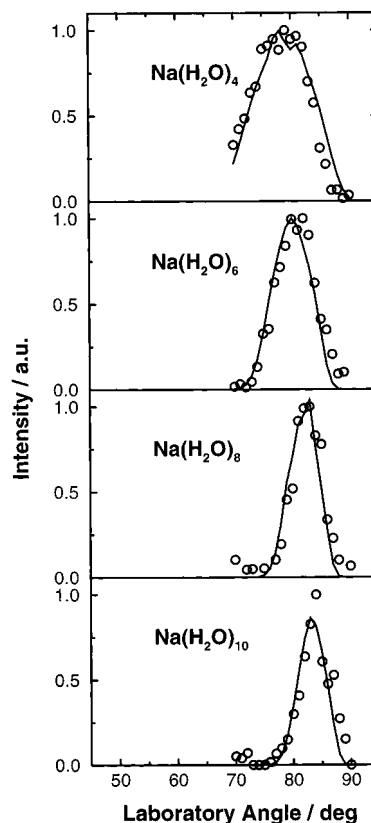


Figure 3. Laboratory angular distribution for different products measured at 308 nm. The solid line represents the distribution calculated with best-fit cm distributions of Figure 7.

alternative reactions for the same product, $\text{Na}_x + (\text{H}_2\text{O})_4 \rightarrow \text{Na}(\text{H}_2\text{O})_4 + \text{Na}_{x-1} + \Delta D$, are all endoergic except for $x = 3$ with $\Delta D = +152$ meV. Therefore, we exclude them for energetic reasons. For the only exothermic reaction with Na_3 as reactant and Na_2 as product, the measured angular and velocity distributions can only be fitted by extreme forward scattering of the product with regard to the water cluster beam, with nearly no internal but high translational energy. The latter result and the small observed cross section is in contrast to the usual spectator stripping model invoked by the forward scattering. In addition, the underlying harpooning mechanism is a very improbable event for this reaction. Therefore, we exclude also this reaction. Similar considerations hold for all other products, and we attribute the formation of the products $\text{Na}(\text{H}_2\text{O})_n$ to Na atoms as reactants. The internal energies of the water clusters do not change this general behavior. The laboratory angular distributions for the products $\text{Na}(\text{H}_2\text{O})_n$, $n = 4, 6, 8$, and 10, at an ionization wavelength of 308 nm are shown in Figure 3. The angular range covered in the measurements is between 70° and 90° . Similar looking angular distributions have been obtained for all the complexes measured. The measurement of the product intensities up to 90° , where they coincide with the direct water cluster beam, is facilitated by the high IP of the pure water clusters, which are not detected by the wavelengths used in the experiment. Clearly, the maximum of the angular distributions falls in the direction of the center of mass for all the products, if the formation of complexes according to eq 1 is assumed. In addition, the product angular ranges are narrow, since the translational energies of the products are only about 20 meV. With increasing size of the complexes, the distributions become narrower and are shifted toward the direction of the direct water cluster beam, as is the position of the center of mass. As was

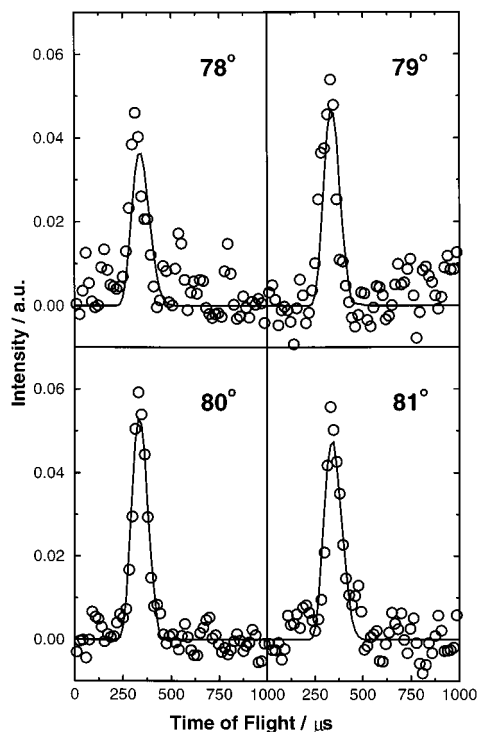


Figure 4. Time-of-flight data of $\text{Na}(\text{H}_2\text{O})_4$ for indicated laboratory angles. Open circles represent the experimental data, and the solid line represents the distribution calculated with best-fit cm distributions of Figure 7.

already mentioned earlier, no difference is observed in the angular distributions measured at an ionization wavelength of 355 nm. The narrow product angular range indicates the formation of reaction products with only a small fraction of the available energy in translation. The angle that corresponds to the center-of-mass (cm) for reactants Na with (H_2O) to $(\text{H}_2\text{O})_{11}$ varies from 39.4° to 82.5° . These values correspond to the angles of maximum intensity of the products, if evaporation of two or three water molecules is assumed. Product time-of-flight distributions have been measured at laboratory scattering angles between 78° and 84° . Figures 4, 5, and 6 depict the time-of-flight distributions of $\text{Na}(\text{H}_2\text{O})_4$, $\text{Na}(\text{H}_2\text{O})_6$, and $\text{Na}(\text{H}_2\text{O})_8$ at different laboratory angles. The laboratory velocity at the maximum of the time-of-flight distribution turns out to be almost constant for all measured laboratory angles and is 1130 , 1078 , and 1130 m s^{-1} for the three products with $n = 4$, 6 , and 8 , within 4% identical with the velocity of the center of mass of the most probable Newton diagrams which give 1108 , 1118 , and 1129 m s^{-1} , respectively. For the interpretation the laboratory angular and velocity distributions (Θ, v) have been transformed to the cm coordinate (θ, u) frame by $I_{\text{lab}}(\Theta, v) = I_{\text{cm}}(\theta, u)v^2/u^2$. Because of the finite resolution of the experiment, the analysis of the laboratory data is carried out by a forward convolution over the experimental conditions of trial cm product flux distributions of angle and translational energy E' of the form

$$I_{\text{cm}}(\theta, E') = T(\theta) P(E') \quad (4)$$

The angular and velocity divergences of the beams, the finite scattering volume, and detector dimensions are all accounted for. The continuous lines in Figures 3–6 are calculated from the best-fit cm distributions which are depicted as solid lines in Figure 7 for $\text{Na}(\text{H}_2\text{O})_4$, $\text{Na}(\text{H}_2\text{O})_6$, $\text{Na}(\text{H}_2\text{O})_8$, and $\text{Na}(\text{H}_2\text{O})_{10}$. The averaged translational energy release is presented in Table 2 together with the reaction and the collision energies. The

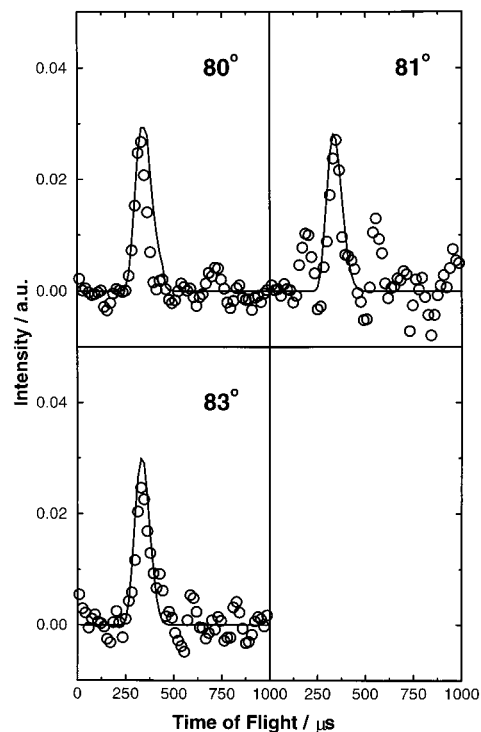


Figure 5. Time-of-flight data of $\text{Na}(\text{H}_2\text{O})_6$ for indicated laboratory angles. Open circles represent the experimental data, and the solid line represents the distribution calculated with best-fit cm distributions of Figure 7.

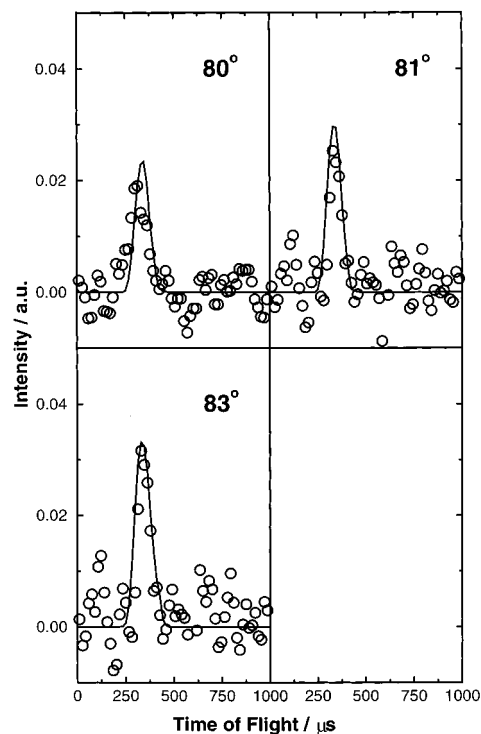


Figure 6. Time-of-flight data of $\text{Na}(\text{H}_2\text{O})_8$ for indicated laboratory angles. Open circles represent the experimental data, and the solid line represents the distribution calculated with best-fit cm distributions of Figure 7.

center-of-mass angular distributions $T(\theta)$ all exhibit a constant cross section corresponding to isotropic evaporation of the water molecules. The center-of-mass translational energy distributions exhibit again the same behavior for all products. Only a very small amount of energy (about 20 meV) is found in the translational energy of the products. This is in agreement with

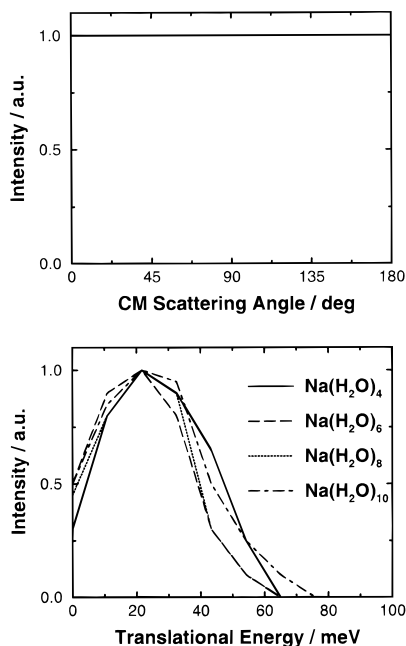


Figure 7. Center-of-mass product angular and translational energy distributions for the indicated reaction products $\text{Na}(\text{H}_2\text{O})_n$ from the reactions $\text{Na} + (\text{H}_2\text{O})_{n+x}$ (for the reactants see Table 2).

TABLE 2: Collision Energies, Reaction Energies, Dissociation Energies, and Averaged Translational and Internal Energies of the Products for Selected Reactions in meV^a

product	reactant	E_{col}	ΔD	$E_{\text{diss}}(\text{H}_2\text{O})$			\bar{E}'_{tr}	\bar{E}'_{int}
				1	2	3		
$\text{Na}(\text{H}_2\text{O})_4$	$(\text{H}_2\text{O})_7$	366	507	270	290	260	26	27
$\text{Na}(\text{H}_2\text{O})_6$	$(\text{H}_2\text{O})_8$	371	403	260	270	(290)	21	223
$\text{Na}(\text{H}_2\text{O})_8$	$(\text{H}_2\text{O})_{10}$	377				(260)	22	
$\text{Na}(\text{H}_2\text{O})_{10}$	$(\text{H}_2\text{O})_{12}$	381					25	

^a The internal energy of the water clusters before the reaction is not included.

the usual values of translational energies at the unimolecular decay of 5–10 meV per evaporated molecule. Since the larger clusters have larger moments of inertia, their angular distributions become narrower at the same translational energies. These findings suggest that a long-lived complex is formed, which is stabilized by isotropic unimolecular evaporation of water molecules, until its internal energy is below its dissociation energy.

4. Discussion

The only products detected are solvated Na atoms in water clusters, $\text{Na}(\text{H}_2\text{O})_n$. We note that both the angular and the velocity distributions are quite narrow. The scattering in the direction of the center of mass is obviously connected with the formation of a long-lived complex that is stabilized by isotropic evaporation of water molecules. This results in small translational energy of the stable complexes which are detected. The product intensities are small, thus indicating small reaction cross sections in the range of 10 \AA^2 . Judging from this result, the reaction equations can be best interpreted by setting $x = 2, 3$ for the production of $\text{Na}(\text{H}_2\text{O})_n$ (see eq 1). Regardless of the number of evaporated water molecules, we observe complexes with small translational energy. The other interpretation, that of a direct reaction involving Na clusters, is apparently ruled out by the fact that they are all endoergic except for Na_3 , which would result in a very improbable reaction mechanism (see

section 3). The fact that no 1:1 $\text{Na}(\text{H}_2\text{O})$ complexes are observed is in agreement with the measurement of Schulz et al.⁹ They found a strong abundance of $\text{Na}(\text{H}_2\text{O})$ and $\text{Na}(\text{H}_2\text{O})_2$, which they, however, attributed to the formation and subsequent cooling by inelastic collisions with the argon carrier gas, whereas they found the larger complexes to be stabilized by evaporative cooling. Under the present single-collision conditions the former way of stabilizing the complexes is ruled out. Although sodium clusters and water clusters were brought together under well-defined conditions, no other reaction products than solvated sodium atoms in water were found. In particular, reaction products that contain NaOH have not been observed under the present experimental conditions. This is, in general, in agreement with the result of the argon–water expansion and the subsequent pickup of sodium atoms under multiple scattering conditions.⁹ It is noted here that a limitation in the search for products is the IP of $(\text{NaOH})_n(\text{H}_2\text{O})_m$, which is probably higher than the photon energies used in the present experiment. On the other hand, these products should be accessible, if additional Na atoms are solvated. This fact will certainly reduce the ionization potential as in the case of the pure water clusters. Some spurious masses observed in ref 9 and attributed to $\text{NaOH}(\text{H}_2\text{O})_n\text{Na}_y$ point into this direction. It seems that the well-known reaction of sodium in liquid water does not proceed in a single collision, at least not within the cluster sizes investigated here. What is known from studies of the decay of hydrated electrons in aqueous alkaline solutions is the existence of neutral solvated metal atoms which react according to $2\text{Na}_{\text{aq}} + 2(\text{H}_2\text{O})_{\text{aq}} \rightarrow 2\text{Na}^+_{\text{aq}} + 2\text{OH}^-_{\text{aq}} + \text{H}_2$ with a rate constant $k = 1.5 \times 10^9 \text{ M}^{-1} \text{ s}^{-1}$, thus confirming an earlier hypothesis.²⁴ This reaction, if it would proceed directly, should in principle be observable in beam experiments. We note that there are two further differences of the beam experiment compared to that in the bulk. Sodium is offered as cluster, not solvated, and the water clusters are solid, not liquid. In a recent theoretical calculation the experimental findings of this work were confirmed. It turned out that the direct reaction $\text{Na}_2 + 2\text{H}_2\text{O} \rightarrow (\text{NaOH})_2 + \text{H}_2$ is forbidden by a barrier of 1.28–1.56 eV depending on the method of calculation.²³ It might well be that similar mechanisms are also operating for the larger clusters investigated here. A possibility to overcome these barriers might be to work with neutral water clusters which contain ionic parts of the type $\text{OH}^-(\text{H}_2\text{O})_n\text{H}_3\text{O}^+$. Such structures have recently been calculated for sizes as small as five water molecules. They require, however, an additional energy of about 0.7–0.9 eV per bond,²⁵ which might not be easy to provide experimentally. While the hope of finding other types of products offering Na clusters and H_2O clusters was not fulfilled, the formation process of the solvated Na atoms in water could be clarified. In fact, the product clusters $\text{Na}(\text{H}_2\text{O})_n$ are interesting species in itself. In two calculations it has been predicted that a change of the behavior occurs with the tetramer $n = 4$, which marks the completion of the first solvation shell. In the calculation using nonlocal pseudopotentials and local-spin-density functional theory, clusters of $n \geq 4$ show a surface delocalized behavior.¹² In the more detailed ab initio molecular orbital study interior and surface states are found, with the latter ones becoming more important for $n \geq 4$. Here in the interior structure the electron density is distributed on and between sodium and the water molecules, while for the surface states the electron is localized in the vicinity of Na opposite to the water molecules.¹³ Spectroscopy on these species should be able to clarify the situation.

5. Summary

The reaction of sodium clusters in the size range $n \leq 21$ with water clusters, $m \leq 40$, is investigated in a crossed molecular beam experiment. By measuring the angular and the velocity distributions of the products, complete information on the reaction mechanisms is obtained. We find only one type of reaction products. These are complexes $\text{Na}(\text{H}_2\text{O})_n$, $2 \leq n \leq 32$, with $n = 4, 5, 6$ as products of largest intensity. The reaction takes place by the formation of long-lived complexes $\text{Na}(\text{H}_2\text{O})_x$ which are stabilized by isotropic evaporation of 2 or 3 water molecules. The measured translational energy is small as is expected from cooling by unimolecular decay. Products containing NaOH are not observed, thus indicating that these products are not formed in single collisions.

Acknowledgment. This work was supported by the Deutsche Forschungsgemeinschaft and the European Community Network "Collision Induced Cluster Dynamics" No. CHRX-CT94-0643. We thank P. Casavecchia for providing us with the program for calculating the center-of-mass variables.

References and Notes

- (1) See several articles in: *Clusters of Atoms and Molecules I*; Haberland, H., Ed.; Springer: Berlin, 1995.
- (2) Dao, P. D.; Peterson, K. I.; Castleman, A. W., Jr. *J. Chem. Phys.* **1984**, *80*, 563. Peterson, K. I.; Dao, P. D.; Castleman, A. W., Jr. *J. Chem. Phys.* **1983**, *79*, 777. Peterson, K. I.; Dao, P. D.; Farley, R. W.; Castleman, A. W., Jr. *J. Chem. Phys.* **1984**, *80*, 1780.
- (3) Brechignac, C.; Cahuzac, Ph.; Carlier, F.; de Frutos, M.; Leygnier, J.; Roux, J. Ph. *J. Chem. Phys.* **1993**, *99*, 6848.
- (4) Martin, T. P. In *Clusters of Atoms and Molecules I*; Haberland, H., Ed.; Springer: Berlin, 1995; p 357.
- (5) Goerke, A.; Leipelt, G.; Palm, H.; Schulz, C. P.; Hertel, I. V. *Z. Phys. D* **1995**, *32*, 311.
- (6) Bewig, L.; Buck, U.; Rakowsky, S.; Reymann, M.; Steinbach, C. *J. Phys. Chem. A* **1997**, *101*, 6538.
- (7) Telsler, T.; Schindewolf, U. *J. Phys. Chem.* **1986**, *90*, 5378.
- (8) Düren, R., unpublished results.
- (9) Schulz, C. P.; Haugstätter, R.; Tittes, H.-U.; Hertel, I. V. *Phys. Rev. Lett.* **1986**, *57*, 1703. Schulz, C. P.; Haugstätter, R.; Tittes, H.-U.; Hertel, I. V. *Z. Phys. D* **1988**, *10*, 279.
- (10) Hertel, I. V.; Huglin, C.; Nitsch, C.; Schulz, C. P. *Phys. Rev. Lett.* **1991**, *67*, 1767.
- (11) Dhar, R.; Kestner, N. R. *Radiat. Phys. Chem.* **1988**, *32*, 355. Dhar, R.; Kestner, N. R. In *Large Finite Systems*; Jortner, J., et al., Eds.; Reidel: Dordrecht, 1987; p 209.
- (12) Barnett, R. N.; Landman, U. *Phys. Rev. Lett.* **1993**, *70*, 1775. Barnett, R. N.; Yannouleas, C.; Landman, U. *Z. Phys. D* **1993**, *26*, 119.
- (13) Hashimoto, K.; Morokuma, K. *J. Am. Chem. Soc.* **1994**, *116*, 11436.
- (14) Herschbach, D. *Faraday Discuss. Chem. Soc.* **1973**, *55*, 233.
- (15) Lee, Y. T. *Science* **1987**, *263*, 793.
- (16) Bewig, L.; Buck, U.; Mehlmann, C.; Winter, M. *J. Chem. Phys.* **1994**, *100*, 2765.
- (17) Bewig, L.; Buck, U.; Gandhi, S. R.; Winter, M. *Rev. Sci. Instrum.* **1996**, *67*, 1.
- (18) Buck, U.; Hoffmann, G.; Kesper, J.; Otten, D.; Winter, M. *Chem. Phys.* **1988**, *126*, 159.
- (19) Bewig, L.; Buck, U.; Mehlmann, Ch.; Winter, M. *Rev. Sci. Instrum.* **1992**, *63*, 3936.
- (20) Watts, R. O., private communication. See also: *The Chemical Physics of Atomic and Molecular Clusters*; Scoles, G., Ed.; North-Holland: Amsterdam, 1990; p 271.
- (21) Knochenmuss, R.; Leutwyler, S. *J. Chem. Phys.* **1992**, *96*, 5233.
- (22) Poteau, R.; Spiegelman, F. *Phys. Rev. B* **1992**, *45*, 1878.
- (23) Barnett, R. N.; Landmann, U. *J. Phys. Chem.* **1996**, *100*, 13950.
- (24) Gopinathan, C.; Hart, E. J.; Schmidt, K. H. *J. Phys. Chem.* **1970**, *74*, 4169.
- (25) Tozer, D. J.; Chengteh Lee; Fitzgerald, G. *J. Chem. Phys.* **1996**, *104*, 5555.